Pergamon

Int. J. Multiphase Flow Vol. 22, Suppl., pp. 1–19, 1996

0301-9322/96 $15.00 + 0.00

S0307-9322(96)00016-X

REGIME TRANSITIONS: ANALOGY BETWEEN GAS–LIQUID CO-CURRENT UPWARD FLOW AND GAS–SOLIDS UPWARD TRANSPORT

H. T. BI† and J. R. GRACE‡

Department of Chemical Engineering, University of British Columbia, Vancouver, Canada V6T 1Z4

(*Received 5 October 1995, in revised form 10 March 1996*)

Abstract—Flow regime transitions in gas–liquid co-current upward transport are analyzed by analogy to gas–solids upward transport. The transition from bubbly flow to slug flow of gas–liquid transport is well predicted by extending an analysis used for gas–solids systems. The transition from slug to churn flow in gas–liquid systems is analogous to the transition from slugging to turbulent fluidization. The transition velocity in gas–liquid systems based on visual observation is found to be close to the point where the maximum of the standard deviation of absolute pressure fluctuations reaches a maximum, the criterion commonly employed to define the onset of turbulent fluidization. The transition from churn to annular flow is also analogous to the transition from fast fluidization to dilute pneumatic transport in gas–solids systems. The data on transition from churn to annular flow is analyzed systematically and compared with available correlations. © 1997 Elsevier Science Ltd.

Key Words: two-phase flow, flow regime transition, gas–liquid upward transport, gas–solids upward transport, fluidization

1. INTRODUCTION

Many flow regime maps have been proposed to delineate the flow patterns of gas–liquid co-current upward flow (e.g. see Hewitt 1977) and gas–solids upward transport (e.g. see Bi and Grace 1995). Table 1 lists the flow regimes identified in gas–liquid vertical upward flow systems by successive authors. It is seen that these maps usually include the bubbly flow, slug flow, churn flow, annular flow and mist flow regimes. Bubbly flow has been further divided into dispersed bubbly flow and coalescing bubbly flow. Churn flow has also been called churn-turbulent flow, froth flow and intermittent flow, while annular flow at high liquid flow rates has been considered as wispy-annular flow, semi-annular flow, ripple flow, wave entrainment and wavy flow due to the appearance of rolling surface waves. Some maps do not consider churn flow as a distinct flow regime, instead treating the whole region between annular flow and bubble flow as the slug flow regime. Some maps further divide bubbly flow into a dispersed bubbly flow and a coalesced bubbly flow regime. In the present analysis, gas–liquid co-current upflow is considered to be composed of four distinct regimes—bubbly flow, slug flow, churn flow and annular flow.

One of the important characteristics of gas–solid fluidized beds is the liquid-like flow behaviour of the dense phase. This character has been widely recognized and used to analyze such gas–solid fluidized bed behaviour as the flowability of gas–solid mixtures (Davidson 1991), phase-equilibrium-like behaviour (Gelperin and Einstein 1973), particle elutriation (Gugnoni and Zenz 1980), apparent viscosity (Grace 1970), bubble motion (Davidson *et al.* 1977) and particle exchange between the core and the annular regions in circulating fluidized beds (Senior and Brereton 1992). There is also an analogy between flow patterns in gas–solids upward transport and gas–liquid upward transport lines (Grace 1986). As shown in figure 1, the flow patterns for gas–liquid co-current upflow lines are strikingly similar to the flow regimes commonly identified in gas–solids vertical transport. In this paper, the analogy of flow regime transitions in gas–liquid two-phase

†Current address: Départment de génie chimique, Ecole Polytechnique, Montréal, Canada.
‡To whom correspondence should be addressed.

Table 1. Summary of proposed flow regimes in the two-phase flow literature

Source	Flow regimes					
Gosline (1936)	Bubble		Slug		Annular	Liquid dispersed
Cromer and Huntington (1940)	Bubble	Slug	Froth	Annular		
Bergelin (1949)	Bubble		Slugging	Annular		
Radford (1949)	Slug		Mixed frothy	Wall-film		Mist
Calvert and Williams (1955)	Aerated	Piston	Churn	Wave-entrainment	Annular	Drop-entrainment
Galegar *et al.* (1954)	Aerated	Slug	Turbulent	Semi-annular	Annular	
Govier *et al.* (1957)	Bubble	Slug	Froth	Ripple	Film	Mist
Duns and Ros (1963)	Bubble	Slug	Transition	Annular		
Wallis (1969)	Bubble		Slug	Annular		Drops
Govier and Aziz (1972)	Bubble	Slug	Froth	Annular		
Oshinowo and Charles (1974)	Bubbly	Slug	Froth	Annular		Mist
Spedding and Nguyen (1980)	Bubble		Intermittent	Wavy	Annular	Mist
Hewitt (1977)	Bubble	Slug	Churn	Wispy-annular		Annular
Taitel *et al.* (1980)	Bubble	Slug	Churn	Annular		Mist
Weisman and Kang (1981)	Bubble	Plug	Churn	Annular		
Vince and Lahey (1982)	Bubble	Slug	Churn	Annular		
Mishima and Ishii (1984)	Bubble	Slug	Churn	Annular		
Annunziato and Girardi (1985)	Bubble	Slug	Churn	Wispy-annular		Annular
Bilicki and Kestin (1987)	Bubble	Slug	Froth	Annular		Mist

co-current upward transport and gas–solids fluidization and upward transport are reviewed and examined by comparing the transition criteria for both types of system.

2. TRANSITION FROM DISPERSED TO COALESING BUBBLE FLOW

When gas is introduced into a liquid, bubbles are generated. The size of bubbles detaching from the bubble generator depends on the diameter of the holes as well as on the gas and liquid properties and the gas flow rate. If the bubbles formed are very small (e.g. several millimeters) and separated by a sufficient distance, they rise vertically with little interaction with each other. Bubbles then do not coalesce to form larger bubbles during their rise. This is generally considered as dispersed bubbly flow. When the superficial gas velocity is increased, both the frequency and the diameter of bubbles increase. Bubbles with smaller separation distances tend to coalesce to form larger ones during their rise. As a result, bubbles start to deviate from their vertical path and migrate toward the axis of the column (Fan *et al.* 1992). Significant internal liquid circulation is set up, with the flow pattern transforming from dispersed bubbly flow to the coalescing bubble regime. With a further increase in superficial gas velocity, significant bubble coalescence occurs right above the

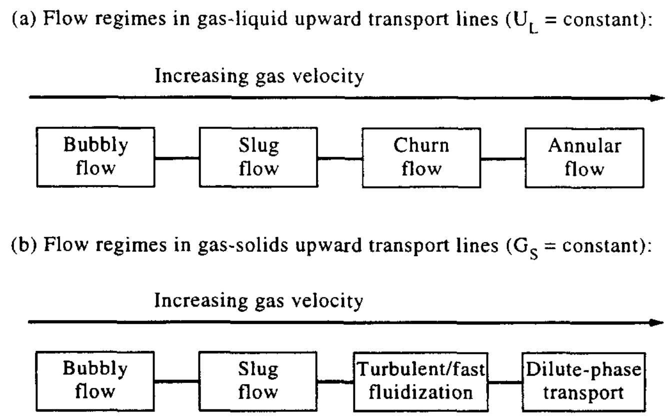

Figure 1. Schematic showing sequence of typical flow patterns observed in: (a) gas–liquid vertical upward transport lines: (b) gas–solids vertical upward transport lines.

distributor. Internal circulation then becomes well established, with large bubbles primarily moving through the core region while liquid descends along the annular region.

In gas–solids fluidized beds, bubbles usually grow by coalescence as they rise. However, for fine (Group A) particles there exists a bubble-free fluidization regime for superficial gas velocities, U, between the minimum fluidization velocity, U_{mf}, and the minimum bubbling velocity, U_{mb}. In this region, small disturbances do not develop into bubbles or voids of significant size. The minimum bubbling velocity, U_{mb}, can be considered to be analogous to the transition velocity from dispersed bubbly flow to the coalescing bubble regime in gas–liquid bubble columns. The bubble-free fluidization regime is then analogous to the dispersed bubble flow regime where small bubbles or "voids" do not coalesce with each other. Such an analogy was examined by Krishna *et al.* (1993).

Figure 2(a) shows typical bed expansion curves for both Group A particles fluidized by a gas. As the superficial gas velocity is increased, the bed starts to expand when the superficial gas velocity exceeds the minimum fluidization velocity and reaches a maximum close to the minimum bubbling velocity. U_{mb} (and the corresponding bed height, H_{mb}) can thus be determined based on the bed expansion curve. In a gas–liquid bubble column, as indicated in figure 2(b), gas holdup or void fraction starts to increase as soon as gas is introduced into the column. With increasing superficial gas velocity, bubble phase holdup increases and reaches a peak at U_{GC} before decreasing. Visually (Hills 1974; Maruyama *et al.* 1981; Fan *et al.* 1992; Tsuchiya and Nakanishi 1992), bubbles are observed to begin to deviate from their vertical path as the bubble holdup begins to level off; some larger bubbles then form due to bubble coalescence, leading to liquid circulation. However, significant bubble coalescence does not appear until the bubble holdup reaches its maximum. As in gas–solids systems, the superficial gas velocity corresponding to the maximum bubble holdup point can be used to indicate the transition from dispersed bubbly flow to the coalescing bubble regime (Verschoor 1950; Tsuchiya and Nakanishi 1992).

The non-dispersed bubble flow regime has been called the "coalescing bubbly flow" regime (e.g. Tsuchiya and Nakanishi 1992), "turbulent bubbly flow" (e.g. Deckwer 1992), "churn turbulent flow" (e.g. Krishna *et al.* 1993) and the "liquid circulation" regime (e.g. Maruyama *et al.* 1981). In view of the analogy to flow patterns in gas–solids fluidized beds, we prefer the term "coalescing

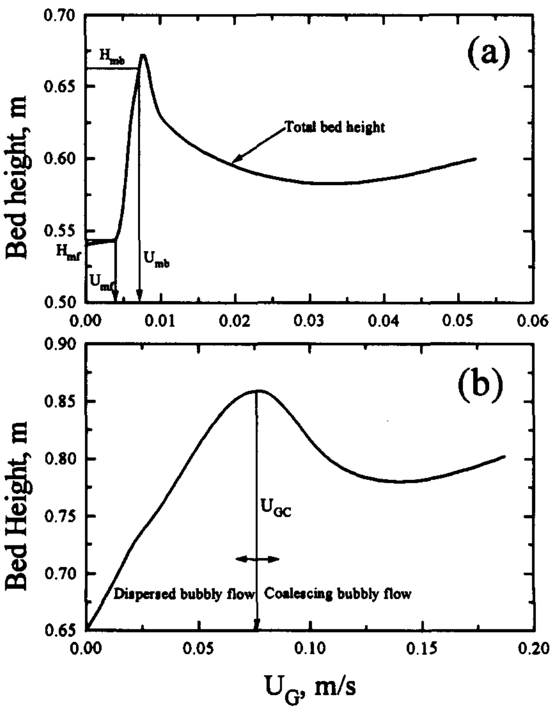

Figure 2. Typical expansion curves for (a) a gas–solids fluidized bed (Abrahamsen and Geldhart 1980) and (b) a gas–liquid bubble column (Maruyama *et al.* 1981).

bubble flow" for the regime between dispersed bubble flow and slug flow, while the term "churn turbulent flow" identifies the regime between slug flow and the annular flow regime.

The analogy between the dispersed bubbly flow and homogeneous fluidization is also reflected in the bed collapse curves from both gas–solids bubbling beds and gas–liquid bubble columns. Figure 3(a) and (b) show typical bed collapse curves of Abrahamsen and Geldart (1980) and Schumpe and Grund (1986) for gas–solids and gas–liquid systems, respectively. In the fluidized bed, the initial sharp decrease in bed height is attributed to the escape of bubbles. In gas–liquid bubble columns operated in the coalescing flow regime the initial sharp decrease in bed height is associated with the escape of fast rising large bubbles. Following the sharp decrease is a linear section corresponding to the escape of the dense phase gas in fluidized beds and the escape of small bubbles in bubble columns. Eventually, the bed height asymptotically approaches H_{mf}, the bed height at minimum fluidization.

The minimum bubbling velocity in gas–solids fluidized bed systems is affected by the distributor design, column size and static bed height (Richardson 1971; Ip 1988). U_{mb} is higher for gas distributors of small hole size, large diameter or lower static bed height. For gas–liquid systems, Verschoor (1950), Freedman and Davidson (1969), Maruyama *et al.* (1981) and Tsuchiya and Nakanishi (1992) found that the transition velocity, U_{dc}, is very sensitive to the hole size and the fractional open area of the distributor. The transition occurred at a much higher gas velocity for perforated plates having small orifices (holes smaller than 0.5 mm diameter) or for porous plates. U_{dc} increases with increasing open area fraction for a fixed hole size by increasing the number of holes (Tsuchiya and Nakanishi 1992). The spatial distribution of holes in the distributor also has some effect on U_{dc} (Maruyama *et al.* 1981). U_{dc} has also been found to decrease with the static height of liquid and to be higher in two-dimensional columns than in three-dimensional vessels (Maruyama *et al.* 1981).

The delineation of the transition from dispersed to coalescing bubbly flow is important for the design of bubble columns. To achieve efficient gas–liquid contact, large gas bubbles should be avoided. Therefore, gas–liquid bubble columns are generally operated within the dispersed bubble regime at low superficial gas velocities with bubble diameter smaller than 10 mm. The fraction of the expanded volume occupied by gas bubbles is typically 10–30%. For gas–liquid heat exchangers, encountered in the energy industry, the column diameter is generally smaller than 50 mm while the

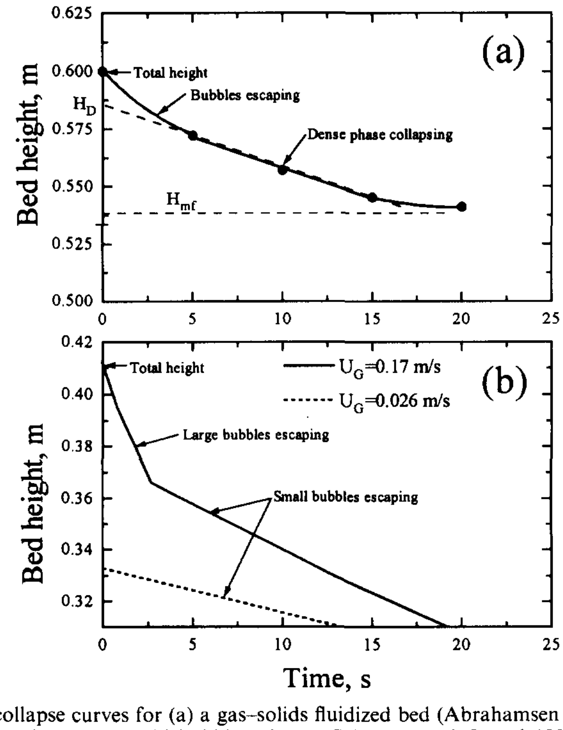

Figure 3. Typical collapse curves for (a) a gas–solids fluidized bed (Abrahamsen and Geldhart 1980) and (b) a gas–liquid bubble column (Schumpe and Grund 1986).

height is several meters. Gas and liquid are generally pre-mixed before entering the column. Under these conditions, the transition velocity U_{dc} is very small, with large bubbles found at the entrance. Therefore, the dispersed bubbly flow regime is unlikely to exist unless the system is operated at a high superficial liquid velocity (Taitel *et al.* 1980).

3. TRANSITION FROM BUBBLY FLOW TO SLUG FLOW

The transition to slug flow is related to the growth of gas bubbles. The transition is considered to occur when gas bubbles grow to be comparable in diameter to the diameter of the column. In a gas–liquid bubble column, the bubble rise velocity, U_B, is related to the superficial gas velocity, U_G, by

$$U_B = U_G/\epsilon \quad [1]$$

where ϵ is the bubble volume fraction. To define the transition, most investigators have sought an expression for the bubble rise velocity and the bubble volume fraction at the transition point. Based on instability of bubble packing, Taitel *et al.* (1980) proposed that the transition from bubbly flow to slug flow occurs when the ϵ reaches 0.25. Mishima and Ishii (1984), on the other hand, considered the transition to occur at $\epsilon \approx 0.30$. Experimentally, Jones and Zuber (1975) found that the transition from bubbly to slug flow occurred for $\epsilon \approx 0.20$ and was insensitive to the liquid flow rate. Barnea and Shemer (1989) reported that $\epsilon \approx 0.24$ at the transition point, while Das and Pattanayak (1994) found that $\epsilon \approx 0.34$ for a small column of diameter $D = 11$ mm.

The bubble rise velocity is, in general, a function of the bubble rise velocity in isolation and the superficial velocity of the liquid, U_L, and of the gas. According to Taitel *et al.* (1980),

$$U_B = (U_G + U_L)/(1 - \epsilon) + 1.53\left[\frac{g\sigma(\rho_L - \rho_G)}{\rho_L^2}\right]^{1/4}. \quad [2]$$

Here ρ_L is the liquid density, ρ_G the gas density and σ the surface tension. By substituting [2] and $\epsilon = 0.25$ into [1], Taitel *et al.* (1980) obtained an equation for the prediction of U_{MS}, the transition superficial velocity from bubbly to slug flow:

$$U_{MS} = 0.5U_L + 0.574\left[\frac{g\sigma(\rho_L - \rho_G)}{\rho_L^2}\right]^{1/4}. \quad [3]$$

Mishima and Ishii (1984), on the other hand, proposed

$$U_B = C_0(U_L + U_G) + \sqrt{2}\left[\frac{\sigma g(\rho_L - \rho_G)}{\rho_L^2}\right]^{1/4}(1 - \epsilon)^{1.75} \quad [4]$$

with $C_0 = 1.2 - 0.2\sqrt{\rho_G/\rho_L}$ for round tubes and $C_0 = 1.35 - 0.35\sqrt{\rho_G/\rho_L}$ for rectangular ducts. Substitution of [4] with $\epsilon = 0.30$ into [1] led to

$$U_{MS} = [C_0/(3.33 - C_0)]U_L + 0.76/(3.33 - C_0)\left[\frac{\sigma g(\rho_L - \rho_G)}{\rho_L^2}\right]^{1/4}. \quad [5]$$

A more complicated equation was derived by Bilicki and Kestin (1987) by assuming that there is a critical separation distance between successive dispersed bubbles beyond which they become unstable. The resulting transition appears, however, to be close to that from [3].

Equations [3] and [5] predict that there is no influence of column size on the onset velocity of slug flow because the rise velocity of isolated bubbles is based on [2], with no allowance for wall effects. However, Hsu and Dudukovic (1980) and Bilicki and Kestin (1987), using columns of different diameter, found experimentally that U_{MS} increased with increasing column diameter, a trend which is consistent with the correlations of Weisman and Kang (1981) and Tutu (1984).

In gas–solids fluidized beds, Stewart and Davidson (1967) considered that (i) the gas slug length is equal to the column diameter, (ii) $\epsilon = 1/6$ based on the assumption that the separation distance

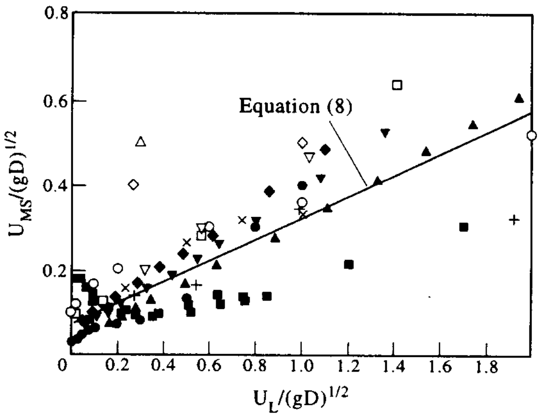

Figure 4. Comparison of experimental data from the literature for onset of slug flow regime with [8]. See table 2 for symbols.

between successive slugs is twice the column diameter and (iii) $U_B = (U - U_{mf}) + 0.35\sqrt{gD}$ to obtain

$$U_{MS} = U_{mf} + 0.07\sqrt{gD} \qquad [6]$$

at the onset of slugging fluidization. In gas–liquid systems with high Reynolds number (based on tube diameter, liquid or gas superficial velocity and liquid kinematic viscosity), the slug rise velocity can be estimated (Grace and Clift 1979) from

$$U_B = 1.2(U_L + U_G) + 0.35\sqrt{gD}. \qquad [7]$$

This equation has been tested by several investigators (see Orell and Rembrand 1986) and gives a good fit for low-viscosity liquids. By substituting U_B from [7] and $\epsilon = 1/6$ into [1], one obtains

$$U_{MS} = 0.25U_L + 0.073\sqrt{gD}. \qquad [8]$$

Figure 4 compares the transition velocity data in the air–water columns listed in table 2 with [8] for column diameters from 19 to 92 mm. It is seen that [8] gives reasonable agreement with most data. Agreement is especially favourable with the data of Hsu and Dudukovic (1980) which are based on the definition that the onset of slugging occurred when the bubble length reached the column diameter, the same assumption as adopted by Stewart and Davidson (1967) for gas–solid systems. This supports the contention that the transition in gas–liquid bubble columns occurs in a manner similar to that in gas–solids fluidized beds.

Table 2. Summary of experimental data for onset of slug flow regime in air–water upflow systems

Source	D (mm)	H (m)	Method†	Symbol in figure 4
Govier *et al.* (1957)	26	9.0	V	◇
Ueda (1958)	50	1.5	V	▽
Griffith and Wallis (1961)	25.4	N/A	V	■
Spedding and Nguyen (1980)	45	N/A	V	△
Hsu and Dudukovic (1980)	19.1	N/A	V	▲
	31.8		V	▼
	40.4		V	◆
Taitel *et al.* (1980)	51	8.4	V	□
Vince and Lahey (1982)	25.4	N/A	X-ray	○
Tutu (1984)	52.2	2.5	P	+
Annunziato and Girardi (1985)	92	3	OP	●
Barnea *et al.* (1985)	51	10	V	×
Barnea (1987)	51	N/A	V	–

†V: Visual observation; X-ray: X-ray measurements; P: pressure fluctuations; OP: optical fibre probe.

4. TRANSITION FROM SLUG FLOW TO CHURN FLOW

The churn or churn-turbulent flow regime has long been proposed as a flow regime located between the slug flow and annular flow regimes (Taitel *et al.* 1980). Such a regime has also been referred to as froth flow (Oshinowo and Charles 1974) and intermittent flow (Weisman and Kang 1981). The churn flow regime is characterized by a chaotic flow pattern and by the disappearance of well-defined liquid or gas slugs. Several mechanism have been proposed to model this transition. Mishima and Ishii (1984) postulated that flow becomes unstable due to the strong wake effect when gas slugs are lined up such that the tail of each preceding slug just touches the nose of the following slug, leading to a transition to churn flow. Brauner and Barnea (1986) attributed the transition to aeration of liquid plugs between the gas slugs. It was postulated that when the gas holdup within the liquid plug reaches a maximum volumetric concentration ($\epsilon = 0.52$), local agglomeration of small bubbles within the highly aerated liquid results in the destruction of the liquid bridge, leading to a transition to churn flow. Taitel *et al.* (1980) considered the transition to result from an entrance effect, postulating that in short columns (e.g. $H < 1$ m), slugs cannot develop fully before erupting at the upper bed surface; the developing slug flow at high gas velocities then appears as churn flow. Such a criterion, however, cannot explain the transition observed in tall columns (Owen 1986; Brauner and Barnea 1986) where fully developed slug flow is attained in the upper region. McQuillan and Whalley (1985), Bilicki and Kestin (1987), Govan *et al.* (1991) and Jayanti and Hewitt (1992) attributed the onset of churn flow to flooding. According to Nicklin and Davidson (1962), the stability of gas slugs is limited by flooding of the film of liquid falling around ascending slugs, with the onset of churn flow corresponding to flooding of the falling liquid film. Flooding of falling liquid film around a rising gas slug was experimentally identified recently by Jayanti *et al.* (1993). After flooding occurs, large gas slugs were said to split into smaller ones, resulting in the breakdown of well-developed slug flow.

Experimental data for evaluating these proposed mechanisms lack consistency due to the absence of a quantitative criterion. All data have been based on visual observation of flow patterns in transparent tubes (Oshinowo and Charles 1974; Taitel *et al.* 1980; Govan *et al.* 1991). The onset superficial gas velocity of the churn flow regime, determined visually by the breakdown of coherent slugs and the appearance of chaotic motion, ranges from 0.5 to 3 m/s for air–water systems operated at ambient temperature and pressure (see table 3). However, it is difficult to distinguish churn flow from slug flow based on visual observation at high superficial liquid velocities. As a result, there are significant discrepancies between different investigations. Data of Nishikawa *et al.* (1965), Govier *et al.* (1957), Hewitt and Roberts (1969) and Owen (1986) indicate that the transition velocity increases with increasing superficial liquid velocity, while data from other investigators (Sternling 1965; Taitel *et al.* 1980; Annunziato and Girardi 1985) suggest that the transition velocity either decreases or remains unchanged with increasing U_L. To quantify this transition, some appropriate criterion is needed, based on measurements of hydrodynamic features like pressure fluctuations or local voidage fluctuations.

In gas–solids systems, the early stage of transition from slugging to turbulent fluidization is commonly defined (see Bi 1994) by the transition velocity U_c at which the standard deviation of

Table 3. Sources of experimental data on onset velocity of churn flow, U_{MC} in air–water systems

Author	D (mm)	H (m)	P (kPa)	Symbol in figure 6 v	Symbol in figure 6 p
Govier *et al.* (1957)	26	9.0	100	◇	
Govier and Short (1958)	16	6.9	250	×	
	64	6.9	250	■	
Brown *et al.* (1960)	16	6.9	256	△	
	38	6.9	128	+	
Chaudhry *et al.* (1965)	25	NA	100		▼
Nishikawa *et al.* (1969)	26	5.2	100	○	●
Hewitt and Roberts (1969)	31.8	NA	100	✱	
Annunziato and Girardi (1985)	92	3.0	100	△	▲
Owen (1986)	32	20.0	230	□	
Mao and Dukler (1993)	51	8.4	100	◆	

v: Visual observation; p: pressure fluctuations.

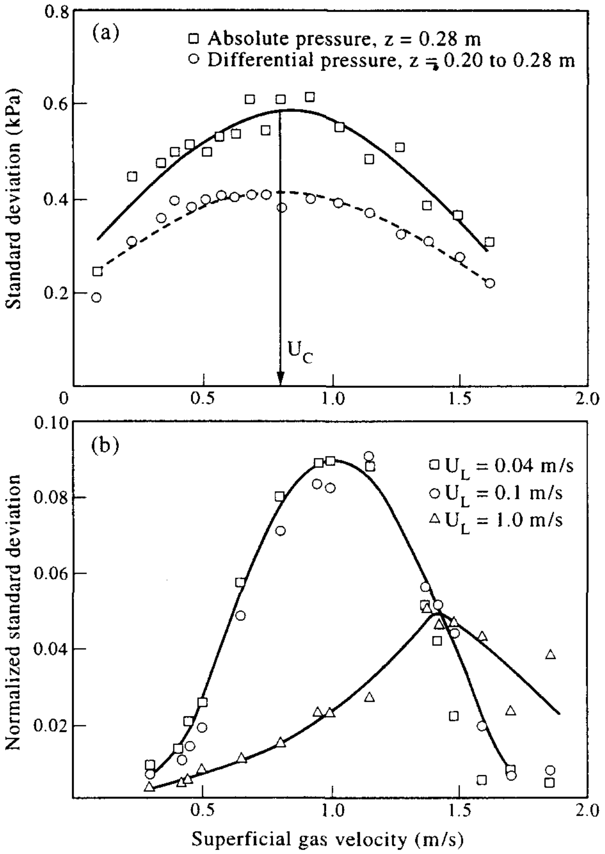

Figure 5. Standard deviation of pressure fluctuation as a function of superficial gas velocity in (a) a gas–solids fluidized bed (Bi and Grace 1995), with z designating the height above the gas distibutor, and (b) a gas–liquid transport line (Annunziato and Girardi 1985).

absolute or differential pressure fluctuations reaches a maximum value [see figure 5(a)]. Absolute and differential pressure fluctuations in gas–liquid bubbly flow systems have been studied by several researchers (Chaudhry *et al.* 1965; Nishikawa *et al.* 1969; Tutu 1982; Matsui 1984; Annunziato and Girardi 1985; Zhang 1996). The transition gas velocity U_{MC} at which the standard deviation of absolute or differential pressure fluctuations reaches a maximum can be identified from a plot of the standard deviation of pressure fluctuations versus superficial gas velocity as shown in figure 5(b). U_{MC} data determined in this manner are plotted against superficial liquid velocity in figure 6. For comparison, data reported in the literature for the transition to churn flow based on

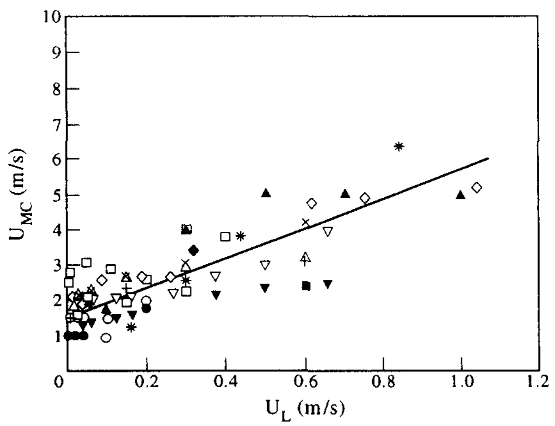

Figure 6. U_{MC} as a function of U_L based on literature data. See table 3 for symbols.

visual observations are also plotted in figure 6. It is seen that the transition velocity based on visual observations is quite close to U_{MC}. The scatter in figure 6 can be attributed to effects of column diameter and gas density, as well as the subjectivity involved in defining the point of transition when visual observations are used as the basis. Govier and Short (1958) reported that U_{MC} tends to decrease with increasing column diameter for D ranging from 16 to 63.5 mm. Brown *et al.* (1960) found that U_{MC} decreased with increasing gas phase density. U_{MC} in steam–water (Bergles and Sou 1966; Hosler 1968) and oil–water (Govier *et al.* 1961) systems has been found to be much lower than in air–water systems, due to smaller density differences between the two phases. These trends are consistent with gas–solids fluidization systems (Bi and Grace 1995). In addition, in gas–solids fluidization systems, U_c based on the standard deviation of differential pressure fluctuations has been determined to be different from that based on absolute pressure fluctuations (Bi and Grace 1995). Similar results have been found in gas–liquid systems (Zhang 1996). Due to the propagation of pressure waves in gas–liquid upflow systems, absolute pressure fluctuations reflect global fluctuations, while differential pressure fluctuations represent relatively localized information (Nishikawa *et al.* 1969). Differential pressure fluctuation measurements are thus recommended for the determination of the transition from bubbly/slug to churn flow.

The transition from slug flow to churn flow can also be quantified based on local voidage fluctuations using X-ray facilities and conductivity probes. The probability distribution function (PDF) of signals has been found to show distinctly different shapes in the different flow regimes (Jones and Zuber 1975; Vince and Lahey 1982; Liu 1993; Das and Pattanayak 1993). In the bubbly flow regime, only one peak appears, corresponding to the liquid phase, while a bimodal distribution appears when slug flow is present in the system. With increasing superficial gas velocity, the amplitude of the peak corresponding to the void phase increases, while that corresponding to the dense phase decreases. Eventually, the peak corresponding to the dense phase disappears when the flow pattern transforms into the annular flow regime. The point where the amplitudes or areas of the two peaks are equal can be adopted as the boundary between the slug flow and churn flow regimes (Vince and Lahey 1982; Das and Pattanayak 1993). It can be shown theoretically that the standard deviation of signals reaches a maximum and the skewness goes to zero at this point, while the void phase volume fraction is 0.5. This is consistent with the experimental data of Vince and Lahey (1982) who measured local voidage fluctuations using an X-ray facility and found that the standard deviation of local voidage fluctuations reached a maximum at $\epsilon = 0.50$, while the skewness of local voidage fluctuations was close to zero. Such an approach is consistent with the absolute pressure fluctuation method and supports the postulate that the probe is covered equally and alternatively by the gas phase and the liquid phase at $U_G = U_{MC}$, consistent with results for gas–solids fluidization (Bi *et al.* 1995b).

There has been some controversy about the existence of a turbulent regime in gas–solids fluidized beds which exhibit slugging and regarding the possibility of churn flow beyond slug flow in gas–liquid transport lines. For gas–solids slugging fluidized beds of large particles, Kehoe and Davidson (1970), Thiel and Potter (1977) and Crescitelli *et al.* (1978) appeared to believe that there is no turbulent regime beyond slugging fluidization. Kunii and Levenspiel (1991) labelled the flow pattern in slugging systems of large particles the "churn turbulent" regime to differentiate it from the "turbulent" regime in non-slugging systems. Bi and Fan (1992) argued that a "fully developed turbulent" regime does not exist in slugging systems involving coarse particles. Mei *et al.* (1991), on the other hand, referred to "apparent slugging", an extension of the "slugging" regime at lower superficial gas velocities because slug-like flow behaviour persists at gas velocities much higher than U_c in slugging fluidized beds of Groups B and D particles (Lee and Kim 1988; Brereton and Grace 1992; Mei *et al.* 1991). A similar argument has been raised (Mao and Dukler 1993; Hewitt and Jayanti 1993) for gas–liquid slug flow. Mao and Dukler (1993) demonstrated that churn flow is simply a manifestation of slug flow and applied a slug flow analysis due to Fernandes *et al.* (1983). On the other hand, Hewitt and Jayanti (1993) argued that a churn flow regime characterized by the breakdown of slugs due to slug–slug interactions (Mishima and Ishii 1984; Bilicki and Kestin 1987; Mao and Dukler 1993) may not exist, but another type of churn flow resulting from flooding of the liquid film surrounding the slug (Hewitt *et al.* 1985; Govan *et al.* 1991; Jayanti *et al.* 1993) does exist, but at a much higher superficial gas velocity. These findings suggest that turbulent fluidization or churn flow in both gas–solids and gas–liquid slug flow systems is simply a transition region between slug flow and annular flow, or an extension of the slug flow regime.

5. TRANSITION FROM CHURN FLOW TO ANNULAR FLOW

In the bubbly, slug and churn flow regimes liquid is either stationary or is introduced from the bottom and overflows from the top because the gas velocity is not high enough to entrain the liquid. When the annular flow regime is reached, a liquid film climbs along the wall of the column so that there is gas–liquid co-current upflow. In a typical operation liquid is introduced into the middle section of a long vertical column and is collected from both the top and the bottom of the column, while gas is introduced only at the bottom. At low gas velocity and low liquid feed rate, liquid flows freely as an annular film downward to the bottom, while gas travels upward in the core in stable counter-current flow. By increasing the gas velocity, a critical condition is encountered when the counter-current flow becomes unstable because of the breakdown of the downflowing liquid film due to the growth of surface waves. As shown by Clift *et al.* (1966) and Wallis (1969) [see figure 7(a)], the pressure drop measured below the liquid feed level increases dramatically with a further increase in superficial gas velocity beyond the critical point due to an abrupt increase in liquid holdup. This critical point is called the "flooding" point, and it marks the termination of stable–liquid counter-current flow (Clift *et al.* 1966).

With a further increase in superficial gas velocity while the liquid flow rate is maintained constant, the pressure drop decreases after passing through a maximum while more and more liquid is carried upward by the gas. Eventually, downflow of liquid ceases at U_{MA} and the lower part of the column begins to dry out. U_{MA} roughly corresponds to the inflection point in the curve of pressure drop against gas flow rate. Such a point is also encountered when the superficial gas velocity is reduced. In the co-current upward annular flow regime, the liquid film flows upwards adjacent to the wall, while gas flows in the center carrying entrained liquid droplets. When the gas velocity is reduced below U_{MA}, called the "flow reversal" point (Hewitt 1977), the gas velocity in the core region becomes insufficient to carry the entrained droplets. Liquid introduced in the middle section of the column then falls back. As a result, liquid accumulates at the bottom unless it is

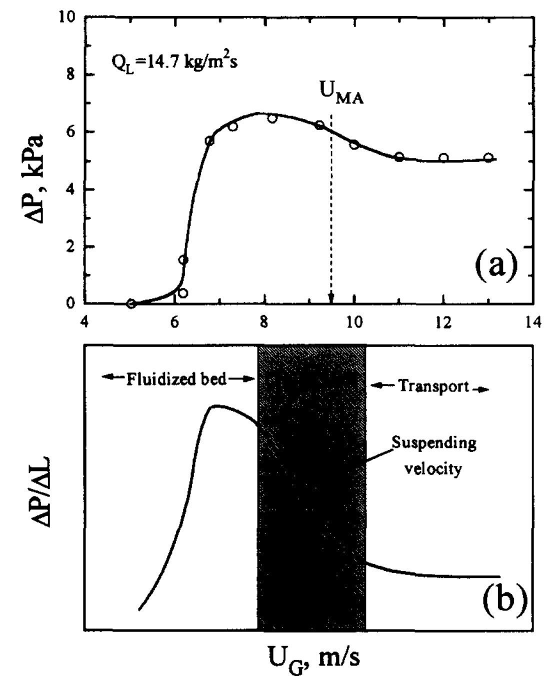

Figure 7. Pressure drop as a function of superficial gas velocity for (a) a counter-current gas–liquid flow system (Clift *et al.* 1966) and (b) a counter-current gas–solids flow system (Wilhelm and Valentine 1957).

discharged there. The core-annular flow structure thus breaks down, and the flow transforms from annular flow to churn flow (Wallis 1969; Taitel *et al.* 1980; McQuillan and Whalley 1985).

A test similar to the flooding and flow reversal test in gas–liquid vertical upflow systems was conducted in gas–solids systems by Wilhelm and Valentine (1951). Spherical clay particles of diameter 5 mm were introduced from a side port into a vertical tube, enabling particles to move freely either upward or downward. As shown in figure 7(b), the pressure profile is similar to that in gas–liquid systems. At low gas velocities, all particles fell downward, while the pressure drop in the bottom section was very low. With increasing gas velocity, the pressure drop began to increase sharply and the suspension density at the lower section increased because the particles were then suspended or fluidized in the lower section. With a further increase in gas velocity, the lower part of the column was maintained fluidized and the pressure drop decreased after passing through a maximum. Particles started to move upward when the gas velocity reached the "suspending velocity" which corresponded approximately to the inflection point of the curve. This suspending velocity was found to be close to the single particle terminal velocity for the large particles used in their tests.

Figure 8(a) and (b) show typical pressure drop versus superficial gas velocity curves at constant liquid and solids flow rates in gas–liquid and gas–solids co-current upward flow systems, respectively. It is seen that the "flow reversal" in gas–liquid systems is analogous to Type A choking in gas–solids fluidized beds (Bi *et al.* 1993, 1995a) in which, with decreasing gas velocity, the gas–solids suspension collapses and particles start to move downwards counter-current to an upflowing gas stream, accumulating at the bottom of the riser. This type A choking velocity in gas–solids vertical transport lines sets the lowest limit of co-current upward fully suspended flow or the boundary between the "turbulent flow" or fast fluidization regime and the dilute-phase transport regime. In an analogous manner for gas–liquid systems, the "flow reversal" velocity sets the lowest limit of the co-current upward transport or the boundary between the churn flow and annular flow regimes.

As shown above, the transition from churn flow to annular flow can be identified either by increasing or decreasing the superficial gas velocity, i.e. from a flooding test or from a flow reversal test. The flow reversal velocity can be determined simply by reducing the superficial gas velocity,

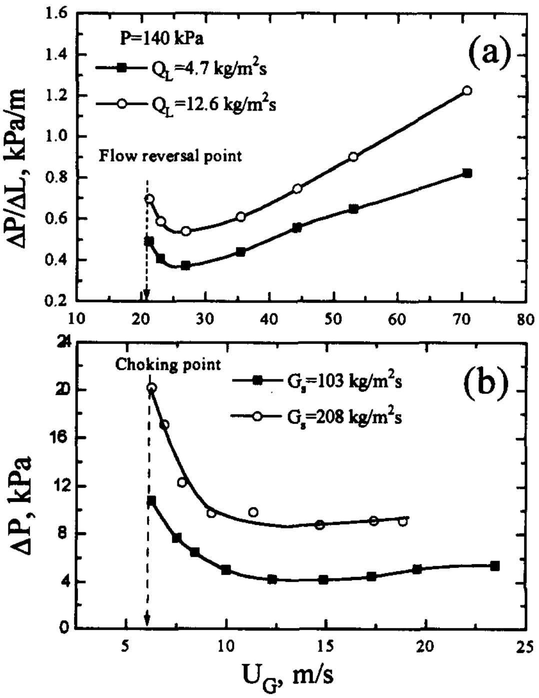

Figure 8. Pressure drop as a function of superficial gas velocity in (a) a co-current gas–liquid upward flow system (Hewitt *et al.* 1965) Q_L and G_S are the net upwards mass flux of the liquid and solids, respectively, and (b) a co-current gas–solids upward transport system (Knowlton and Bachovchin 1976).

because flow reversal is insensitive to the liquid flow rate (Hewitt *et al.* 1965; Clift *et al.* 1966; Wallis and Makkenchery 1974). On the other hand, the flooding velocity increases with decreasing liquid flow rate, with the flow reversal velocity, U_{MA}, corresponding to where the liquid flow rate approaches zero (Clift *et al.* 1966; Chaudhry *et al.* 1965; Suzuki and Ueda 1977). Table 4 presents

Table 4. Summary of U_{MA} data for atmospheric pressure air–liquid vertical flow systems

Source	D (mm)	Liquid	σ (N/m)	$\mu_L \times 10^{-3}$ (Pa/s)	U_{MA} (m/s)	Method
Bashforth *et al.* (1963)	31.8	Water	0.073	1.1	9.5	F
Nicklin and Davidson (1962)	31.8	Water	0.073	1.1	9.5	FR
Hewitt *et al.* (1965)	31.8	Water	0.073	1.1	11.8	F
Clift *et al.* (1966)	31.8	Water	0.073	1.1	10.7	F and FR
	31.8	Glycerol	0.072	1.3	10.3	
	31.8	Glycerol	0.068	2.2	10.1	
	31.8	Glycerol	0.067	10.4	10.0	
	31.8	Glycerol	0.066	11.8	10.1	
	31.8	Glycerol	0.066	23.4	9.9	
	31.8	Glycerol	0.065	44.8	10.0	
	31.8	Glycerol	0.065	82.5	10.0	
Stainthorpe and Batt (1967)	26	Water	0.073	1.1	10.5	F
Wallis (1969)	22.2	Water	0.073	1.1	11.0	F
	22.2	Glycerol	0.073	9.0	9.1	
	22.2	Glycerol	0.073	39.0	7.6	
	22.2	Glycerol	0.073	60.0	7.9	
	22.2	Glycerol	0.073	116	7.9	
	22.2	Glycerol	0.073	498	7.9	
	22.2	Glycerol	0.073	1270	7.9	
	22.2	Glycerol	0.073	3000	7.8	
Pushkina and Sorokin (1969)	6.2	Water	0.073	1.1	14.5	FR
	8.8	Water	0.073	1.1	14.5	
	9	Water	0.073	1.1	15.0	
	13	Water	0.073	1.1	15.0	
	13	Water	0.073	1.1	16.0	
	30.2	Water	0.073	1.1	15.5	
	309	Water	0.073	1.1	15.5	
Wallis and Makkenchery (1974)	19	Water	0.073	1.1	7.0	FR
	38	Water	0.073	1.1	10.3	
	51	Water	0.073	1.1	11.5	
	64	Water	0.073	1.1	10.9	
	76	Water	0.073	1.1	10.2	
	89	Water	0.073	1.1	10.7	
	100	Water	0.073	1.1	9.4	
	140	Water	0.073	1.1	6.5	
Suzuki and Ueda (1977)	18	Water	0.073	1.1	11.0	F and FR
	10	Water	0.073	1.1	11.0	
	28.8	Water	0.073	1.1	12.0	
Hewitt (1977)	31.8	Water	0.018	0.82	9.4	F
	31.8	Silicone oil	0.067	18.0	9.8	
	31.8	Glycerol	0.073	1.1	8.4	
Imura *et al.* (1977)	11.2	Water	0.073	1.1	9.0	F
	16	Water	0.073	1.1	9.5	
	21	Water	0.073	1.1	9.5	
	11.2	*n*-Heptane	0.020	4.1	6.0	
	16	*n*-Heptane	0.020	4.1	7.0	
	21	*n*-Heptane	0.020	4.1	9.0	
	24.2	*n*-Heptane	0.020	4.1	9.0	
	11.2	Ethyl-alcohol	0.024	—	7.5	
	16	Ethyl-alcohol	0.024	—	8.2	
	21	Ethyl-alcohol	0.024	—	8.5	
	11.2	Ethylene-glycol	0.063	—	7.0	
	16	Ethylene-glycol	0.063	—	9.0	
	24.2	Ethylene-glycol	0.063	—	9.5	
Richter (1981)	25.4	Water	0.073	1.1	8.3	FR
	50.8	Water	0.073	1.1	11.8	
	152	Water	0.073	1.1	14.2	
	254	Water	0.073	1.1	15.1	
Taitel *et al.* (1980)	51	Water	0.073	1.1	15.0	F
Govan *et al.* (1991)	31.8	Water	0.073	1.1	11.3	F

†F—flooding tests; FR—flow reversal tests.

U_{MA} data from the literature from flow reversal tests and those evaluated based on flooding velocity data from the literature. U_{MA} is seen to be of order 10 m/s in all cases.

To verify whether U_{MA} corresponds to the transition from churn to annular flow, data on the transition from churn flow to annular flow in gas–liquid co-current upflow systems are listed in table 5. It is seen that the transition from churn to annular flow has usually been visualized to occur at a superficial gas velocity around 10 m/s in atmospheric pressure air–liquid systems. The agreement of the former with the atmospheric data listed in table 4 suggests that the transition from churn to annular flow may well correspond to U_{MA}.

To predict this transition, Taitel *et al.* (1980) considered the onset of entrainment of liquid droplets in the gas core, and derived an equation to predict the minimum gas velocity required to suspend a droplet based on a balance between gravity and drag forces on a liquid drop, leading to

$$U_{MA} = K[\sigma g(\rho_L - \rho_G)]^{1/4}/\rho_G^{1/2}. \qquad [9]$$

A value of 3.1 was suggested for the constant K by Taitel *et al.* (1980). A similar equation was derived by Pushkina and Sorokin (1969), although with a slightly different constant, $K = 3.2$. Mishima and Ishii (1984) considered the instability of the upflowing liquid film and derived the following equation for the transition from churn to annular flow,

$$U_{MA}[gD(\rho_L - \rho_G)/\rho_G]^{1/2}(\epsilon - 0.11). \qquad [10]$$

The void fraction at this transition point, ϵ, is generally around 0.8.

This transition can also be predicted theoretically by simply applying the flooding velocity correlations at zero liquid flow rate (Wallis 1969; McQuillan *et al.* 1985). A popular flooding equation due to Wallis (1969) relates the liquid and gas flow rates at the flooding point by

$$U_G^{*1/2} + U_L^{*1/2} = C^{1/2} \qquad [11]$$

where C is a constant whose value is of order unity, and U_G^* and U_L^* are defined by

$$U_G^* = U_G[\rho_G/gD(\rho_L - \rho_G)]^{1/2} \qquad [12]$$

$$U_L^* = U_L[\rho_L/gD(\rho_L - \rho_G)]^{1/2}. \qquad [13]$$

U_{MA} can thus be calculated from [11] by taking U_L^* as zero, leading to

$$U_{MA} = C[gD(\rho_L - \rho_G)/\rho_G]^{1/2}. \qquad [14]$$

Here C ranges from 0.5 to 1.0, depending on the tube end conditions and the tube length (Wallis 1969; McQuillan *et al.* 1985). An alternative equation was proposed by Richter (1981), which includes the effects of both column diameter and surface tension, i.e.

$$Ku^2 = -75[1 - (1 + D^{*2}/75^2/C_w)^{1/2}]/D^* \qquad [15]$$

Table 5. Summary of the boundary between churn and the annular flow regimes in atmospheric pressure air–water systems

Source	D (mm)	Transition velocity† (m/s)
Govier *et al.* (1957)	26	9.5
Nishikawa *et al.* (1964)	26	9.5
Oshinowo and Charles (1974)	26	8.0
Taitel *et al.* (1980)	25	9.5
	51	10.0
Vince and Lahey (1982)	25.4	2.3
Tutu (1982)	52.2	11.8
Shoham (1982)	12.5	8.0
	25.0	10.5
Annunziato and Girardi (1985)	92	9.5

†Transition velocity delineating the boundary between the churn and annular flow regimes in co-current upward flow systems.

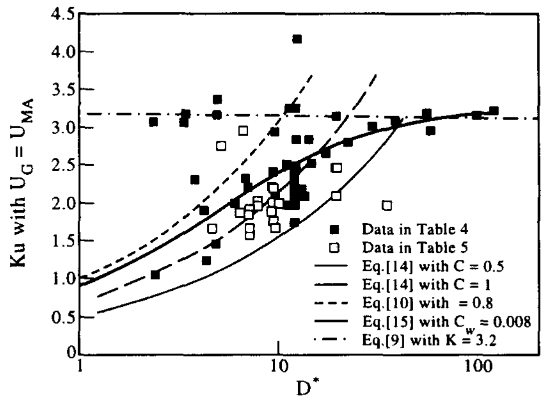

Figure 9. Comparison of U_{MA} data from the literature with available empirical correlations. Data sources are listed in tables 4 and 5.

where $D^* = D[(\rho_L - \rho_G)g/\sigma]^{1/2}$ is the Bond number, $Ku = U_G\rho_G^{1/2}/[(\rho_L - \rho_G)g\sigma]^{1/4}$ is the Kutateladze number and C_W, the wall friction factor, is approximately equal to 0.008.

Comparison of the experimental data in table 4 with [9], [10], [14] and [15] is shown in figure 9 with the Bond number plotted against the Kutateladze number, as recommended by Wallis and Makkenchery (1974). Equation [15] shows good agreement with most experimental data. All four equations predict that U_{MA} is inversely proportional to the square root of gas density. This is supported by the experimental data obtained at various system pressures by Hewitt *et al.* (1965), Bergles and Suo (1966) and McQuillan *et al.* (1985), as listed in table 6. All four equations predict that the liquid phase viscosity does not affect U_{MA}, consistent with the experimental data of Clift *et al.* (1966) and Wallis (1969). Equations [10] and [14] predict an increase of U_{MA} with increasing column diameter, while [9] indicates that column diameter has no effect on U_{MA}, and [15] suggests that D has some influence for small columns, but not for large diameter columns. Experimentally, Wallis and Makkenchery (1974) and Ritcher (1981) reported that U_{MA} increased with column diameter but became insensitive in large columns. The data of Pushkina and Sorokin (1969), on the other hand, showed that U_{MA} was insensitive to column diameter for $6 < D < 300$ mm. The data in figure 5 suggest that U_{MA} increases with column size, at least for small columns ($D^* < 30$). Equation [9] predicts that U_{MA} increases with surface tension. The limited data of Hewitt *et al.* (1965) and Imura *et al.* (1977), do suggest that U_{MA} depends on the surface tension. Until more experimental data are available to evaluate these equations further, [15] is recommended for the estimation of U_{MA}.

The annular flow regime can be further divided into two sub-regimes, annular flow proper and wispy-annular flow. Only small drops are present in the core on the former, while larger drops or liquid streamers are present in the core for wispy-annular flow. In general, wispy-annular flow is encountered at high superficial liquid velocities when the upflowing liquid film is thick and large waves are generated at the core–annular interface. Annular flow is, however, observed at low liquid flow rates with small waves generated at the interface of thin liquid films. No systematic work has been carried out to provide a quantitative boundary between these two sub-regimes, although the

Table 6. Summary of U_{MA} data for high pressure gas–liquid vertical flow systems

Source	D (mm)	Liquid	Gas	P (kPa)	U_{MA} (m/s)
Chaudhry *et al.* (1965)	25.4	Water	Air	200	7.2
Hewitt *et al.* (1965)	31.8	Water	Air	140	11.7
	31.8	Water	Air	280	8.9
McQuillan *et al.* (1985)	31.8	Water	Air	150	13.0
	31.8	Water	Air	133	9.5
	31.8	Water	Air	200	7.8
	31.8	Water	Air	267	6.0
Bergles and Suo (1966)	10	Water	Steam	3400	2.5
				6900	1.7

transition has been suggested to be at a superficial liquid velocity of about 0.1 m/s (Annunziato and Girardi 1985). In this study, we prefer to regard annular flow as a single regime rather than as two sub-regimes.

In the annular flow regime, the liquid film is maintained by drop deposition, while depletion of the film is caused by drop entrainment. There are two opinions about the transition to mist flow. One considers that mist flow is reached when significant drop entrainment occurs, with drops carried upward in the core region by the gas while most of the liquid still rises as a thin film. The other considers that mist flow is reached when the liquid film disappears because the deposition rate cannot balance the entrainment rate. This condition is known as "dryout". For boiling heat transfer, it causes deterioration in the heat transfer coefficient and can lead to a large increase in wall temperature, a potentially hazardous condition in heat flux controlled systems, such as nuclear reactor cooling systems. In gas–solids vertical upward transport, the flow pattern is said to transform from annular flow to homogeneous transport when the superficial gas velocity is increased beyond the minimum pressure point in figure 8(b). Similarly, a minimum pressure drop point exists in figure 8(a) with increasing superficial gas velocity at constant liquid flow rate. This minimum pressure drop point in gas–liquid vertical transport lines can probably be used to define the transition from annular flow to mist flow. However, the dryout condition is seldom encountered in practical operations, while the onset of drop entrainment occurs right after annular flow is reached. Therefore mist flow is not considered a separate regime in this study.

6. CONCLUSIONS

Gas–liquid cocurrent upflow in vertical columns exhibits remarkable similarity with the upward transport of gas and solid particles. The four key hydrodynamics regimes for gas–liquid systems—bubbly flow, slug flow, churn flow and annular flow—have direct counterparts for gas–solids upward transport—bubble flow, slug flow, turbulent/fast fluidization and dilute-phase pneumatic transport. Corresponding flow regimes in the two types of systems are visually rather similar. Moreover, the transitions from one regime to the next appear to involve analogous mechanisms, such that lessons learned in one type of system can be applied to the other. In the early days of study of fluidization, most of the transfer of knowledge was from gas–liquid two-phase systems to achieving an understanding of gas–solids systems. However, given the extent of investigation of gas–solids upwards transport and the scarcity of data for gas–liquid transport involving liquids other than water, it is now possible to apply knowledge in the other direction.

In this paper, we show that the transition from bubbly to slug flow in gas–liquid systems can be predicted by extending the approach proposed by Stewart and Davidson (1967) for gas–solids fluidized beds. The transition from slug to churn flow in gas–liquid vertical transport can be defined on the basis of the standard deviation of pressure fluctuations reaching a maximum value, analogous to the superficial velocity, U_c, commonly used to denote the transition from slug flow to turbulent fluidization in gas–solids systems. Similarly, the transition from churn flow to annular flow in gas–liquid vertical flow is shown to correspond to the "flow reversal velocity", analogous to the type A choking velocity which has been found to delineate the transition between fast fluidization and dilute phase pneumatic transport of solids. Examination of various correlations used to predict the latter transition suggests that the correlation of Richter (1981) gives the best predictions. Since this correlation includes a weak dependence on the gas–liquid surface tension, a property which is absent for gas–solids systems, the analogy does not lead to quantitative predictions. However, the relationship in both cases between the transition and the saturation carrying capacity of the gas is helpful in understanding the nature of the respective transitions.

While the analogies considered herein are between gas–liquid and gas–solid systems, it seems likely that additional analogies may exist involving two-phase liquid–liquid systems and three-phase (gas–liquid–solid and gas–liquid–liquid) systems. These possible analogies will be explored in future work.

REFERENCES

Abrahamsen, A. R. and Geldart, D. (1980) Behaviour of gas-fluidized beds of fine powders. Part II. Voidage of the dense phase in bubbling beds. *Powder Technol.* **26,** 47–55.

Annunziato, M. and Girardi, G. (1985) Statistical methods to identify two-phase regimes: Experimental results for vertical large diameter tubes. In *Proceedings of 2nd Int. Conf. Multiphase Flow*, pp. 361–380, London, England.

Barnea, D. (1987) A unified model for predicting flow-pattern transitions for the whole range of pipe inclinations. *Int. J. Multiphase Flow* **13,** 1–12.

Barnea, D. and Shemer, L. (1989) Void fraction measurements in vertical slug flow: applications to slug characteristics and transitions. *Int. J. Multiphase Flow* **15,** 495–504.

Barnea, D., Shoham, O., Taitel, Y. and Dukler, A. E. (1985) Gas–liquid flow in inclined tubes: flow pattern transitions for upward flow. *Chem. Eng. Sci.* **40,** 131–136.

Bashforth, W. Q., Fraser, J. B. P., Hutchinson, H. P. and Nedderman, R. M. (1963) Two-phase flow in a vertical tube. *Chem. Eng. Sci.* **18,** 41–46.

Bergelin, O. (1949) Flow of gas–liquid mixtures. *Chem. Eng.* **56**(5), 104–107.

Bergles, A. E. and Sou, M. (1966) Investigation of boiling water flow regimes at high pressure. *Proc. 1966 Heat Trans. and Fluid Mech. Inst.*, M. A. Saad, and J. A. Miller), pp. 79–88. Stanford Press, California.

Bi, H. T. (1994) Flow regime transitions in gas–solid fluidization and vertical transport. Ph.D. thesis, University of British Columbia, Canada.

Bi, H. T. and Fan, L.-S. (1992) On the existence of turbulent regime in gas–solid fluidization. *AIChE J.* **38,** 297–301.

Bi, H. T. and Grace, J. R. (1995) Effect of measurement method on the velocities used to demarcate the onset of turbulent fluidization. *Chem. Eng. J.* **57,** 261–271.

Bi, H. T., Grace, J. R. and Zhu, J. X. (1993) On types of choking in pneumatic systems. *Int. J. Multiphase Flow* **19,** 1077–1092.

Bi, H. T., Grace, J. R. and Zhu, J. X. (1995a) Transition velocities affecting regime transitions in gas–solids suspensions and fluidized beds. *Chem. Eng. Res. Des.* **73A,** 154–161.

Bi, H. T., Grace, J. R. and Lim, K. S. (1995b) Transition from bubbling to turbulent fluidization. *Ind. Eng. Chem. Research* **34,** 4003–4008.

Bilicki, Z. and Kestin, J. (1987) Transition criteria for two-phase flow patterns in vertical upward flow. *Int. J. Multiphase Flow* **13,** 283–294.

Brauner, N. and Barnea, D. (1986) Slug/churn transition in upward gas–liquid flow. *Chem. Eng. Sci.* **41,** 159–163.

Brereton, C. M. H. and Grace, J. R. (1992) The transition to turbulent fluidization. *Chem. Eng. Res. Des.* **70,** 246–251.

Brown, R. A. S., Sullivan, G. A. and Govier, G. W. (1960) The upward vertical flow of air–water mixtures: III. Effect of gas phase density on flow pattern, holdup and pressure drop. *Can. J. Chem. Eng.* **38,** 62–66.

Calvert, S. and Williams, B. (1955) Upward cocurrent annular flow of air and water in smooth tubes. *AIChE J.* **1,** 78–86.

Chaudhry, A. B., Emerton, A. C. and Jackson, R. (1965) Flow regimes in the co-current upwards flow of water and air. In *Symp. on Two Phase Flow*, Vol. 1, Univ. of Exeter, Devon, England, pp. B201–208.

Clift, R., Pritchard, C. L. and Nedderman, R. M. (1966) The effect of viscosity on the flooding conditions in wetted wall columns. *Chem. Eng. Sci.* **21,** 87–95.

Crescitelli, S., Donsi, G., Russo, G. and Clift, R. (1978) High velocity behaviour of fluidized beds: slugs and turbulent flow, Chisa Conference, Prague, pp. 1–11.

Cromer, S. and Huntington, R. L. (1940) Visual studies of the flow of air–water mixtures in a vertical pipe. *Trans. Am. Inst. Mining, Met. and Petrol. Engrs* **136,** 79–88.

Das, R. K. and Pattanayak, S. (1993) Electrical impedance method for flow regime identification in vertical upward gas–liquid two-phase flow. *Meas. Sci. Technol.* **4,** 1457–1463.

Das, R. K. and Pattanayak, S. (1994) Bubble to slug flow transition in vertical upward two-phase flow through narrow tubes. *Chem. Eng. Sci.* **49,** 2163–2172.

Davidson, J. F. (1991) The two-phase theory of fluidization: Successes and opportunities. *AIChE Symp. Series* **87**(281), 1–12.

Davidson, J. F., Harrison, D. and Guedes de Carvalho, J. R. F. (1977) On the liquid-like behaviour of fluidized beds. *Ann. Rev. Fluid. Mech.* **9,** 55–86.

Deckwer, W.-D. (1992) *Bubble Column Reactors*. Wiley, New York.

Duns, Jr., H. and Ros, N. C. J. (1963) Vertical flow of gas and liquid mixtures from boreholes. *Proc. 6th World Petroleum Congress*, Section 2, Paper 22, Frankfurt.

Fan, L. S., Tzeng, J. W. and Bi, H. T. (1992) Flow structures in a two-dimensional bubble column and three-phase fluidized beds. In *Fluidization VII*, eds O. E. Potter and D. J. Nicklin). pp. 399–406. Engineering Foundation, New York.

Fernandes, R. C., Semiat, R. and Dukler, A. E. (1983) A hydrodynamic model for gas–liquid slug flow in vertical tubes. *AIChE J.* **29,** 981–989.

Freedman, W. and Davidson, J. F. (1969) Hold-up and liquid circulation in bubble columns. *Trans. Instn Chem. Engrs* **47,** T251–262.

Galegar, W. C., Stovall, W. B. and Huntington, R. L. (1954) More data on two-phase vertical flow. *Petroleum Refiner* **33,** 208.

Gelperin, N. I. and Einstein, V. G. (1973) The analogy between fluidized beds and liquids. Chapter 11 in *Fluidization* J. F. Davidson and D. Harrison. pp. 541–568. Academic Press, London.

Gosline, J. E. (1936) Experiments on the vertical flow of gas–liquid mixtures in glass pipes. *Trans. Am. Inst. Mining, Met. and Petrol. Engrs* **118,** 56–70.

Govan, A. H., Hewitt, G. F., Richter, H. J. and Scott, A. (1991) Flooding and churn flow in vertical pipes. *Int. J. Multiphase Flow* **17,** 27–44.

Govier, G. W. and Short, W. L. (1958) The upward vertical flow of air–water mixtures: II. Effect of tubing diameter on flow pattern, holdup and pressure drop. *Can. J. Chem. Eng.* **36,** 195–202.

Govier, G. W. and Aziz, K. (1972) *The Flow of Complex Mixtures in Pipes*. Van Nostrand-Reinhold, New York.

Govier, G. W., Radford, B. A. and Dunn, J. S. C. (1957) The upwards vertical flow of air–water mixtures, I. Effect of air and water rates on flow pattern, holdup and pressure drop. *Can. J. Chem. Eng.* **35,** 58–70.

Govier, G. W., Sullivan, G. A. and Wood, R. K. (1961) The upward vertical flow of oil–water mixtures. *Can. J. Chem. Eng.* **39,** 67–75.

Grace, J. R. (1970) The viscosity of fluidized beds. *Can. J. Chem. Eng.* **48,** 30–33.

Grace, J. R. (1986) Contacting modes and behaviour classification of gas–solid and other two-phase suspensions. *Can. J. Chem. Eng.* **64,** 353–363.

Grace, J. R. and Clift, R. (1979) Dependence of slug rise velocity on tube Reynolds number in vertical gas–liquid flow. *Chem. Eng. Sci.* **34,** 1348–1350.

Griffith, P. and Wallis, G. B. (1961) Two-phase slug flow. *J. Heat Transfer* **83,** 307–320.

Gugnoni, R. J. and Zenz, F. A. (1980) Particle entrainment from bubbling fluidized beds. In *Fluidization*, eds J. R. Grace and J. M. Matsen). pp. 501–508, Plenum Press, New York.

Hewitt, G. F. (1977) Flow patterns. Chapter 2 in *Two-Phase Flow and Heat Transfer* eds D. Butterworth, and G. F. Hewitt). pp. 18–39, Oxford University Press.

Hewitt, G. F. and Roberts, D. N. (1969) Studies of two-phase flow patterns by simultaneous X-ray and flash photography. UKAEA Report AERE-M2159.

Hewitt, G. F. and Jayanti, S. (1993) To churn or not to churn. *Int. J. Multiphase Flow* **19,** 527–529.

Hewitt, G. F., Lacey, P. M. C. and Nicholls, B. (1965) Transitions in film flow in a vertical tube. In *Symp. on Two Phase Flow*, Univ. of Exeter, Devon, England, Vol. 1, pp. B401–430.

Hills, J. H. (1974) Radial non-uniformity of velocity and voidage in a bubble column. *Trans. Instn Chem. Engrs* **52,** 1–9.

Hosler, E. R. (1968) Flow patterns in high pressure two-phase (steam–water) flow with heat addition. *Chem. Eng. Prog. Symp. Ser.* **64**(82), 54.

Hsu, Y. C. and Dudukovic, M. P. (1980) Liquid recirculation in gas-lift reactors. *Proc. 2nd Multiphase Flow and Heat Transfer Symp.*, ed. T. N. Veziroglu). Vol. 4, 1757–1775. Hemisphere, Washington, Imura, H., Kusuda, H. and Funatsu, S. (1977) Flooding velocity in a countercurrent annular two-phase flow. *Chem. Eng. Sci.* **32,** 79–87.

Ip, T.-L. (1988) Influence of particle size distribution on fluidized bed hydrodynamics. M.Sc. thesis, University of British Columbia, Vancouver, Canada.

Jayanti, S. and Hewitt, G. F. (1992) Prediction of the slug-to-churn flow transition in vertical two-phase flow. *Int. J. Multiphase Flow* **18,** 847–860.

Jayanti, S., Hewitt, G. F., Low, D. E. F. and Hervieu, E. (1993) Observation of flooding in the Taylor bubble of co-current upwards slug flow. *Int. J. Multiphase Flow* **19,** 531–534.

Jones, O. C. and Zuber, N. (1975) The interrelation between void fraction fluctuations and flow patterns in two-phase flow. *Int. J. Multiphase Flow* **2,** 273–306.

Kehoe, P. W. K. and Davidson, J. F. (1970) Continuously slugging fluidized beds, Chemeca '70. *Inst. Chem. Eng. Symp. Ser.*, No. 33, Butterworths, Australia, pp. 97–116.

Krishna, R., Ellenberger, J. and Hennephof, D. E. (1993) Analogous description of the hydrodynamics of gas–solid fluidized beds and bubble columns. *Chem. Eng. J.* **53,** 89–101.

Kunii, D. and Levenspiel, O. (1991) *Fluidization Engineering*, 2nd edition. Butterworth-Heinemann, Boston, MA.

Lee, G. S. and Kim, S. D. (1988) Pressure fluctuations in turbulent fluidized beds. *J. Chem. Eng. Japan* **21,** 515–521.

Liu, T. J. (1993) Bubble size and entrance length effects on void development in a vertical channel. *Int. J. Multiphase Flow* **19,** 99–113.

Mao, Z. S. and Dukler, A. E. (1993) The myth of churn flow. *Int. J. Multiphase Flow* **19,** 377–383.

Maruyama, T., Yoshida, S. and Mizushina, T. 1981 The flow transition in a bubble column. *J. Chem. Eng. Japan* **14,** 352–357.

Matsui, G. (1984) Identification of flow regimes in vertical gas–liquid two-phase flow using differential pressure fluctuations. *Int. J. Multiphase Flow* **10,** 711–720.

McQuillan, K. W. and Whalley, P. B. (1985) Flow patterns in vertical two-phase flow. *Int. J. Multiphase Flow* **11,** 161–175.

McQuillan, K. W., Whalley, P. B. and Hewitt, G. F. (1985) Flooding in vertical two-phase flow. *Int. J. Multiphase Flow* **11,** 741–760.

Mei, J. S., Rockey, J. M., Lawson, W. F. and Robey, E. H. (1991) Flow regime transitions in fluidized beds of course particles. *Proc. 11th Int. Fluidized Bed Combustion Conf.*, ed. E. J. Anthony), pp. 1225–1232, A.S.M.E. New York.

Mishima, K. and Ishii, M. (1984) Flow regime transition criteria for upward two-phase flow in vertical tubes. *Int. J. Heat Mass Transfer* **27,** 723–737.

Nicklin, D. J. and Davidson, J. F. (1962) The onset of instability in two-phase slug flow. Presented at *Int. Mech. Engr. Symp. on Two-Phase Flow*, Exeter, Devon.

Nishikawa, K. Sekoguchi, K. and Fukano, T. (1969) Characteristics of pressure pulsation in upward two-phase flow. In *Co-current Gas–Liquid Flow*, eds E. Rhodes and D. S. Scott). Plenum Press, New York, pp. 18–46.

Orrel, A. and Rembrand, R. (1986) A model for gas–liquid slug flow in a vertical tube. *Ind. Eng. Chem. Fundam.* **25,** 196–206.

Oshinowo, T. and Charles, M. E. (1974) Vertical two-phase flow. Part I: Flow pattern correlations. *Can. J. Chem. Eng.* **52,** 25–35.

Owen, D. G. (1986) An experimental and theoretical analysis of equilibrium annular flows. Ph.D. thesis, Univ. of Birmingham, U.K.

Pushkina, O. L. and Sorokin, Y. L. (1969) Breakdown of liquid film motion in vertical tubes. *Heat Transfer—Soviet Research* **1,** 56–64.

Radford, B. A. (1949) M.Sc. thesis, Univ. of Alberta.

Richardson, J. F. Incipient fluidization and particulate systems. Chapter 2 in *Fluidization* eds J. F. Davidson and D. Harrison). pp. 26–61, Academic Press, London.

Richter, H. L. (1981) Flooding in tubes and annuli. *Int. J. Multiphase Flow* **7,** 647–658.

Schumpe, A. and Grund, G. (1986) The gas disengagement technique for studying gas holdup structure in bubble columns. *Can. J. Chem. Eng.* **64,** 891–896.

Senior, R. C. and Brereton, C. (1992) Modelling of circulating fluidized bed solids flow and distribution. *Chem. Eng. Sci.* **47,** 281–296.

Shoham, O. (1982) Flow pattern transitions and characterization in gas–liquid two phase flow in inclined pipes. Ph.D. thesis, Tel-Aviv University, Ramat-Aviv, Israel.

Spedding, P. L. and Nguyen, T. V. (1980) Regime maps for air–water two-phase flow. *Chem. Eng. Sci.* **35,** 779–793.

Stainthorpe, F. P. and Batt, R. S. W. (1967) The effect of co-current and counter-current air flow on the wave properties of falling liquid film. *Trans. Inst. Chem. Engr.* **45,** T372–T382.

Sternling, V. C. (1965) Two-phase flow theory and engineering decision. Presented at *AIChE* Annual Meeting.

Stewart, P. S. B. and Davidson, J. F. (1967) Slug flow in fluidized beds. *Powder Technol.* **1,** 61–80.

Suzuki, S. and Ueda, T. (1977) Behaviour of liquid films and flooding in counter-current two-phase flow—Part I. Flow in circular tubes. *Int. J. Multiphase Flow* **3,** 517–532.

Taitel, Y., Bornea, D. and Dukler, A. E. (1980) Modeling flow pattern transitions for steady upward gas–liquid flow in vertical tubes. *AIChE J.* **26,** 345–354.

Thiel, W. J. and Potter, O. E. (1977) Slugging in fluidized beds. *Ind. Eng. Chem. Fund.* **16,** 242–247.

Tsuchiya, K. and Nakanishi, O. (1992) Gas holdup behaviour in a tall bubble column with perforated plate distributors. *Chem. Eng. Sci.* **47,** 3347–3354.

Tutu, N. K. (1982) Pressure fluctuations and flow pattern recognition in vertical two phase gas–liquid flows. *Int. J. Multiphase Flow* **8,** 443–447.

Tutu, N. K. (1984) Pressure drop fluctuations and bubble-slug transition in a vertical two phase air–water flow. *Int. J. Multiphase Flow* **10,** 211–216.

Ueda, T. (1958) Studies of the flow of air–water mixtures—the upward flow in a vertical tube. *JSME* **1,** 139–145.

Verschoor, H. (1950) Some aspects of the motion of a swarm of gas bubbles rising through a vertical liquid column. *Trans. Inst. Chem. Engrs* **28,** 52–57.

Vince, M. A. and Lahey, R. T. (1982) On the development of an objective flow regime indicator. *Int. J. Multiphase Flow* **8,** 93–124.

Wallis, G. B. (1969) *One-Dimensional Two-phase Flow.* McGraw-Hill, New York.

Wallis, G. B. and Makkernchery, S. (1974) The hanging film phenomenon in vertical annular two-phase flow. *J. Fluids Eng.* **96**(3), 297–298.

Weisman, J. and Kang, S. Y. (1981) Flow pattern transitions in vertical and upwardly inclined lines. *Int. J. Multiphase Flow* **7,** 271–291.

Wilhelm, R. H. and Valentine, S. (1951) The fluidized bed. *Ind. Eng. Chem.* **43,** 1199–1203.

Zhang, J. P. (1996) Flow regimes and bubble behaviour in bubble columns and three-phase fluidized beds. Ph.D. thesis, University of British Columbia, Vancouver, Canada.